Journal of Physics and Chemistry of Solids 148 (2021) 109614

Contents lists available at ScienceDirect

Journal of Physics and Chemistry of Solids

journal homepage: http://www.elsevier.com/locate/jpcs

Thermophysical properties of magnesium arsenide with atomistic simulation methods

Seçkin D. Günay

Department of Physics, Faculty of Science, Yıldız Technical University, Esenler, 34210, İstanbul, Turkey

ARTICLE INFO

Keywords:
Magnesium arsenide
Lattice parameter
Superionic
Mechanical property
Diffusion

ABSTRACT

A classical interionic potential for the Buckingham potential model was developed for magnesium arsenide (Mg_3As_2). Potential parameters were fitted to available experimental and first-principles data in the literature. They were implemented in classical molecular dynamics programs, and static properties such as lattice constant, bulk modulus, shear modulus, Young's modulus, elastic constants, Poisson's ratio and anisotropy factor were obtained at 0 K. Lattice constants, linear thermal expansion coefficients, heat capacities, self-diffusion coefficients for each axis, bulk moduli and radial distribution functions were calculated from room temperature up to the melting point. A superionic phase transition was observed. The superionic phase transition and the melting temperature points were found ~1505 K and ~1700 K by two-phase simulation box method, respectively. This method was used for the first time to determine the superionic phase transition temperature. Lattice parameter and bulk modulus were also calculated by the first-principles method. All the calculated data displayed an agreement with the available experimental and first-principles data in the literature. The present parameters of Buckingham potential provide a good description of magnesium arsenide (Mg_3As_2) crystal.

1. Introduction

Magnesium arsenide (Mg_3As_2) is one of the members of magnesium pnictides. Pnictogens belong to group 15 in the periodic table. Semiconductor magnesium pnictides are considered good candidates for thermoelectric devices [1]. Magnesium arsenide is a semiconductor with a wide band gap 2.2eV [2] which was studied for the use in electronic and optoelectronic devices. Even though it is considered to be a good candidate for industrial applications, the toxic effect is one of the drawbacks of the material.

Magnesium arsenide (Mg_3As_2) has two types of structural forms. Cubic Mn_2O_3 type is the low-temperature form of the crystal with the space group $Ia\bar{3}$. At about 1000–1100 °C, cubic magnesium arsenide undergoes a phase transition to hexagonal structure, anti- La_2O_3 system with the space group $P\bar{3}m1$. High-temperature hexagonal form melts above 1200 °C [2,3].

To the best of our knowledge, almost all of the theoretical studies on magnesium arsenide were first-principle calculations aiming to investigate electronic structures [4], lattice parameters, enthalpies [5] and mechanical properties [6,7] of the cubic structure. Ground state properties of the hexagonal structure, high-temperature form, of Mg_3As_2 was studied by some groups [6,8]. Tani et al. [8] investigated the lattice dynamics and thermodynamic properties of hexagonal-Mg_3As_2.

In this study, both classical and first-principles methods had been used to examine the Mg_3As_2 crystal structure. Some of the previous ground state calculation results, lattice constant and bulk modulus, had been verified with the first-principles study. Semi-empirical interaction potential parameters were proposed for Mg_3As_2 to perform classical molecular dynamics simulations. Thermodynamic and elastic properties were calculated with molecular dynamics programs and compared with the available data in the literature.

2. Calculation methods

2.1. Potential model

Magnesium pnictides compounds were a poorly studied topic with the classical simulation tools; consequently, a limited number of interaction potentials were developed in the literature such as for Mg_3Bi_2 and Mg_3Sb_2 [9,10]. In this work, Buckingham type interaction potential parameters were developed, and physical properties were obtained for Mg_3As_2. The following expression is a combination of Coulomb and Buckingham interaction potentials,

E-mail address: sgunay@yildiz.edu.tr.

https://doi.org/10.1016/j.jpcs.2020.109614
Received 24 February 2019; Received in revised form 21 May 2020; Accepted 7 June 2020
Available online 26 July 2020
0022-3697/© 2020 Elsevier Ltd. All rights reserved.

$$V_{ij}(r) = \frac{q_i q_j e^2}{4\pi\varepsilon_0} + A_{ij} exp\left(-\frac{r}{\rho_{ij}}\right) - \frac{C_{ij}}{r^6} \quad (1)$$

The Coulomb interaction has charges indicated with sub-indices i and j that refer to anions and cations. The second term is the repulsive part of the potential due to the Pauli Exclusion Principle. Interaction potential may be very attractive at short distances, and non-physical interactions between ions could occur. However, this can be avoided by the second term. The third one is the van der Waals attraction term and can be tuned with the C_{ij} parameter. The parameters, A, ρ and C were obtained by the trial-error method (see Table 1).

Parameters were calculated by fitting to experimental and first-principles data, such as lattice constant, lattice angle, bulk modulus, shear modulus and elastic constants$(C_{11},\ C_{12},\ C_{44})$. Most of the weight is given to the lattice constant among these physical properties. f_i^{calc} is the estimated physical parameter, and f_i^{obs} is the first-principles or the experimental data.

$$F = \sum_{i=1}^{N_{obs}} w_i \left(f_i^{obs} - f_i^{calc}\right)^2 \quad (2)$$

Qualities of the estimated parameters were determined by equation (2) [11]. The cut-off value for the Buckingham potential is 20 Å.

2.2. Procedure

2.2.1. Classical MD method

Magnesium arsenide has two types of structures. First one is the low-temperature phase from room temperature to 1273 K–1373 K. The second one is the high-temperature phase form 1273 K–1373 K to the melting point [3]. The melting point is reported to take place above 1473 K [2,3]. The low-temperature phase has the cubic Mn_2O_3 type structure, and the high-temperature phase has the anti- La_2O_3 type structure. Their space groups are $Ia\bar{3}$ and $P\bar{3}m1$, respectively. In this study, the initial configuration of molecular dynamics programs is the cubic Mn_2O_3 type structure, which is the low-temperature form of the magnesium arsenide molecule. It has 80 ions in its unit cell, 32 of them are the anions (As^{-3}), 48 of them are the cations (Mg^{+2}). Experimental lattice constant is 12.33 Å [2,3,12]. Molecular dynamics simulation supercell box is constructed with 4 × 4 × 4 unit cells. The total number of ions are 5120 (2048 As^{-3} and 3072 Mg^{+2}).

In this study, MOLDY (MD_1) [13] and LAMMPS (MD_2) [14] molecular dynamics programs were used to calculate physical properties. In MD_1 equilibration process were performed for 30 ps by rescaling velocities iteratively to the desired temperature. Constant stress simulation method (Parrinello and Rahman constant stress) was used to allow supercell shape to change size and shape so any phase change-structural, superionic and melting-can be observed. The temperature was kept constant by the coupling the system to a heat bath with the method called Nose-Hoover thermostat. Simulations were carried out from 300 K to 2000K at every 50 K interval. Each of the simulations was 500 ps. NPT simulation was used to calculate the lattice parameters, enthalpies, heat capacities and radial distribution functions at each temperature. Mean square displacement data and diffusion coefficients were obtained from the NVT ensemble that is initiated with the final configuration of the NPT ensemble of the same temperature. Each of the NVT ensemble simulations was also 500 ps. The number of ions in the supercell box of MD_1 was increased (6 × 6 × 6 unit cells) to reduce the vibrations and obtain a more accurate value for bulk modulus versus temperature data, where the total number of ions are 17280 (6912 As^{-3} and 10368 Mg^{+2}).

MD_2 was generally used to verify that the results were program-independent. Lattice parameters and phase transition points of one phase MD box were recalculated with the similar input parameters of MD_1. Instead of rescaling velocities used in MD_1, the steepest descent energy minimization algorithm was applied to the simulation box in MD_2. NPT ensemble was carried out, and the temperature was gradually increased from 300 K to 2000 K for 20000 ps. The superionic phase transition and the melting points were calculated by the two-phase simulation technique with the MD_2 program.

Finally, static calculations were performed with GULP [11] program to obtain lattice constant, elastic constants, compressibility, Poisson's ratio, bulk modulus, shear modulus, Young's modulus, anisotropy factor and B/G ratio. The data obtained from all three programs were examined to see if they were consistent with each other.

2.2.2. First principles method

VASP (Vienna Ab-initio Simulation Package) [15–17] was used to obtain the ground state structure, and energies of cubic Mg_3As_2 molecule with the projector augmented wave method. Generalized gradient approximation using the Perdew–Burke–Ernzerhof (PBE) function was utilized to calculate the exchange-correlation energy. Simulation cell contained 80 ions, where the anion (As^{-3}) number was 32, and the cation (Mg^{+2})number was 48. The cutoff energy for plane wave basis set was 600 eV. The k-point mesh was generated by Monkhorst-Pack technique and fineness was gradually increased. 6 × 6 × 6 were sufficient to obtain results to less than 0.1 meV/atom.

3. Results and discussions

3.1. Static properties

In this part, static properties were initially calculated by searching the energy maps by classical methods which were implemented in the GULP program [11]. Stationary points were found with BFGS energy minimization method. The lattice constant, elastic constants, bulk modulus, shear modulus, Young's modulus, compressibility, Poisson's ratio and anisotropy factor were calculated at T = 0 K when the minimum energy configuration was reached.

Calculated physical properties were compared with available data in the literature. In Table 2, all the physical properties, except the experimental lattice constant, were obtained at T = 0 K. Lattice constant calculated from GULP program was 12.281 Å. In Section 3.2.1, lattice constant from the MD simulation at room temperature will be given and compared with the experimental data.

Table 1
Buckingham type interaction potential parameters. $Z_{As} = -2.04$ and $Z_{Mg} = 1.36$.

	A/eV	ρ/Å	C/eV Å^6
As–As	400.0	0.13636	200.0
As–Mg	992.0434	0.38333	80.0
Mg–Mg	9547.96	0.21916	0.0

Table 2
Lattice constants and mechanical properties of cubic magnesium arsenide in literature were compared with our results.

	Classical (This work)	First-Principles (This work)	First-Principles	Exp.
a_0 (Å)	12.281	12.456	12.455 [5,7] 12.465 [6]	12.33 [2,3,12]
B (GPa)	47.109	49.79	49.4 [7] 50.576 [6]	
G (GPa)	22.701		27.7 [7]	
C_{11} (GPa)	69.284		76.2 [7]	
C_{12} (GPa)	36.021		36.1 [7]	
C_{44} (GPa)	27.961		32.9 [7]	
B/G	2.075		1.78 [7]	
$Mg-As$ (Å)	2.648		2.681 [6]	

Elastic constants (for cubic systems, C_{11}, C_{12}, C_{44}), bulk and shear moduli strongly depend on the shape of the energy surface. They were calculated by applying small finite strains to the crystal structure. Bulk modulus, the resistance of the material to the hydrostatic pressure, was obtained. When the shear stress was implemented on the structure, shear modulus was acquired from its response. Both of these moduli were calculated in three ways; Voigt, Reuss and Hill [18–20]. The third one is the mean value of the first two data. These methods are summarized for cubic structures as follows,

$$B_V = \frac{(C_{11} + 2C_{12})}{3} \tag{3}$$

$$G_V = \frac{(C_{11} - C_{12} + 3C_{44})}{5} \tag{4}$$

$$G_R = \frac{5C_{44}(C_{11} - C_{12})}{4C_{44} + 3(C_{11} - C_{12})} \tag{5}$$

Voigt and Reuss methods for bulk modulus are the same for cubic systems. Thus our calculated results were 47.109 GPa for all three of them. These three methods resulted 21.973 GPa, 23.429 GPa, 22.701 GPa for shear modulus value, respectively (Table 2).

First-principles calculations were also used to acquire ground state lattice constant and bulk modulus values. Ground state lattice constant was obtained with the conjugate-gradient algorithm by initially relaxing ions, and subsequently relaxing ions, cell shape and volume (Table 2).

Hydrostatic pressure was applied to the optimized structure. The equation of state, energy versus lattice parameter, was plotted in Fig. 1. Rose-Vinet equation of state [21] was fitted to the energy data to calculate bulk modulus value.

$$E = -E_c\left(1 + \alpha + 0.05\alpha^3\right)e^{-\alpha} \tag{6}$$

$$\alpha = \sqrt{\frac{9B_o V_o}{E_c}}(x-1), x = (V/V_o)^{1/3} \tag{7}$$

Here, E is the energy, B_0 is bulk modulus, V_0 is the volume of the optimized structure, E_c is the minimum energy. Bulk modulus was calculated 49.79 GPa from equation (6) (Table 2).

B/G ratio, which was proposed by Pugh [22], has a value 2.075 in Table 2 higher than the critical point 1.75, which means that the material displays ductile behavior. Cauchy relation was also used to determine whether the material is ductile or brittle. $C_{12} - C_{44} > 0$ condition indicates the material is ductile. Mechanical stability criteria were established with our available data of elastic constants. For cubic crystals following criteria is present in the literature [23],

$$B = (C_{11} + 2C_{12})/3 > 0, \quad C_{11} > 0, \quad C_{44} > 0, \quad C_{11} - C_{12} > 0 \tag{8}$$

Cubic Mg_3As_2 is considered to be a mechanically stable material from equation (8). Other mechanical properties like Young's modulus, Poisson's ratio, anisotropy factor and compressibility were given in Table 3. Here Zener anisotropy factor is,

$$A = \frac{2C_{44}}{(C_{11} - C_{12})} \tag{9}$$

This value is called the quantity of degree of anisotropy in cubic crystals. Isotropic materials have a value of 1.

Mokhtari et al. [6] calculated nearest neighbor distance 2.681 Å for magnesium – arsenic ions from first-principles. Distances between these two types of ions (As–Mg, Mg–Mg, As–As) were measured from the radial distribution function by the MD simulation method, 2.648 Å, 3.39

Table 3
Young's modulus (E), Poisson's ratio (σ), anisotropy factor (A) and compressibility (β) were calculated for cubic magnesium arsenide.

	$E(GPa)$	σ	A	$\beta(1/GPa)$
This Work (Classical)	44.641	0.3421	1.681	0.0212274

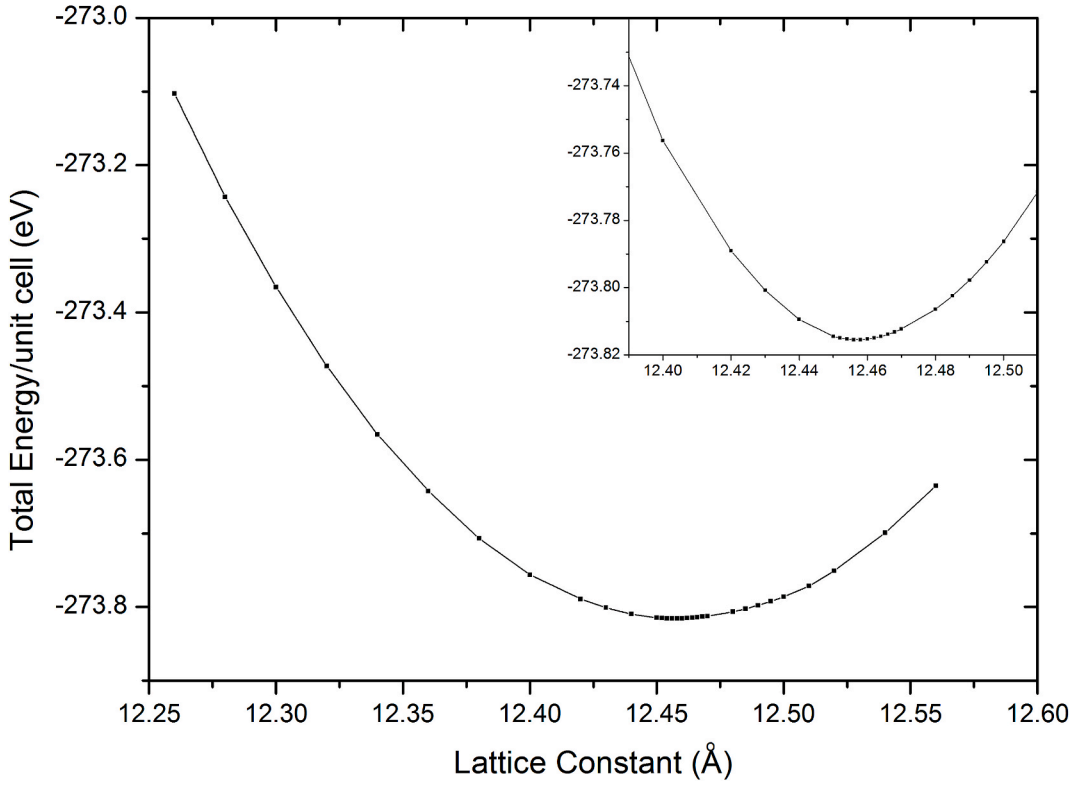


Fig. 1. Total energy versus lattice constant from first-principles calculations for cubic Mg_3As_2.

Å and 4.14 Å, respectively at room temperature. Details of the distribution function were investigated in Section 3.2.4.

3.2. Thermodynamic properties

3.2.1. Lattice parameter

The lattice parameter of the cubic Mg_3As_2 structure was calculated from room temperature to 2000 K. NPT ensemble was applied to the simulation box. Lattice parameters and lattice angles for each axis in three dimensions could change non-uniformly at all temperatures to reveal any phase change in MD_1 and MD_2 [13,14].

Buckingham potential was implemented in two classical MD simulation programs and both of them gave almost same results for lattice constants in three dimensions in Fig. 2. The data obtained from MD simulation programs were 12.329 Å at room temperature, which is in agreement with the experimental value in Table 2. The system had remained solid up to 1950 K. Restoring forces vanished and the system could not sustain shear stress at the melting point, which is 2000 K. MD cell shape evolved rapidly into an elongated shape. Eventually, lattice parameters displayed a discontinuity at the onset of the melting point. Besides, another discontinuity was observed in the lattice constant at 1800 K. A superionic phase transition is observed, where the magnesium sub-lattice demonstrate liquid behavior and the arsenic sub-lattice maintains its solid form. The structural transformation of As sub-lattice that occurred during the superionic phase transition was discussed in section 3.2.7 with diffraction pattern data. In the following sections, other physical data also indicate that the phase transition points are about 1800 K and 2000 K for magnesium arsenide. However, it should be emphasized that one-phase simulations generally overestimate melting points. In Section 3.2.8 "corrected" superionic phase transition and melting points were found with the two-phase simulation method at about 1505 K and 1700 K, respectively. In literature [2,3], experimental melting temperature was estimated as "above 1473 K", so it is roughly compared with the calculated data.

Experimental studies [3] had also showed that between 1273 K and 1373 K cubic magnesium arsenide crystal undergoes a structural phase transition to hexagonal structure (high-temperature form) of an anti--La_2O_3 system. This allotropic phase transition from cubic to hexagonal was not observed with the current potential. This issue will be reconsidered in section 3.2.5.

The following equation relates the lattice constant as a function of temperature in the 300 K–1600 K range,

$$a(T) = 12.28047 + 1.59889 \times 10^{-4} \times T + 3.9686 \times 10^{-9} \times T^2 + 8.81967 \times 10^{-12} \times T^3 \quad (10)$$

The lattice constant is 12.28047 Å from equation (10) at 0 K. This is almost identical to the static calculation value, 12.281 Å, in Table 2.

3.2.2. Thermal expansion coefficient

Linear thermal expansion coefficient is given as,

$$\alpha_P(T) = \frac{1}{L_{300}}\left(\frac{\partial L}{\partial T}\right)_P \quad (11)$$

It could be deduced that linear thermal expansion coefficient data with temperature is a quadratic function (Equations (10) and (11)), and were plotted in Fig. 3. The thermal expansion coefficient of magnesium arsenide at room temperature was found $1.337x10^{-5}(K^{-1})$. In literature,

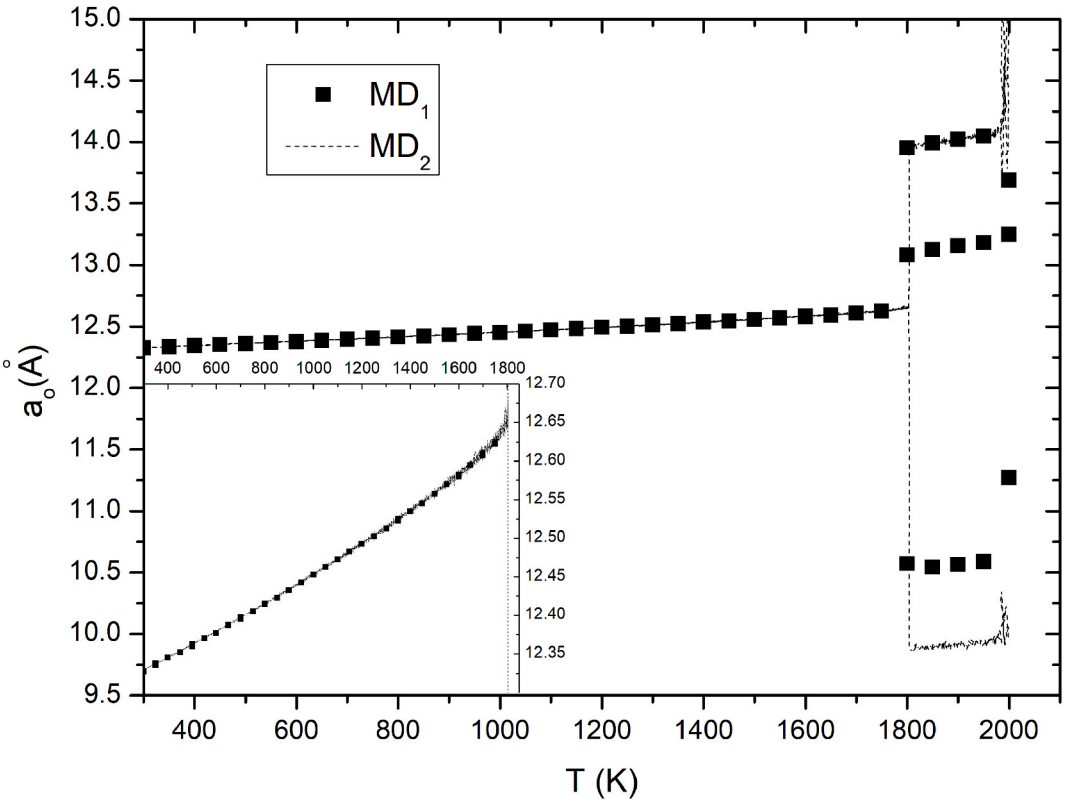


Fig. 2. Components of magnesium arsenide lattice constants was calculated with two different MD simulation programs [13,14].

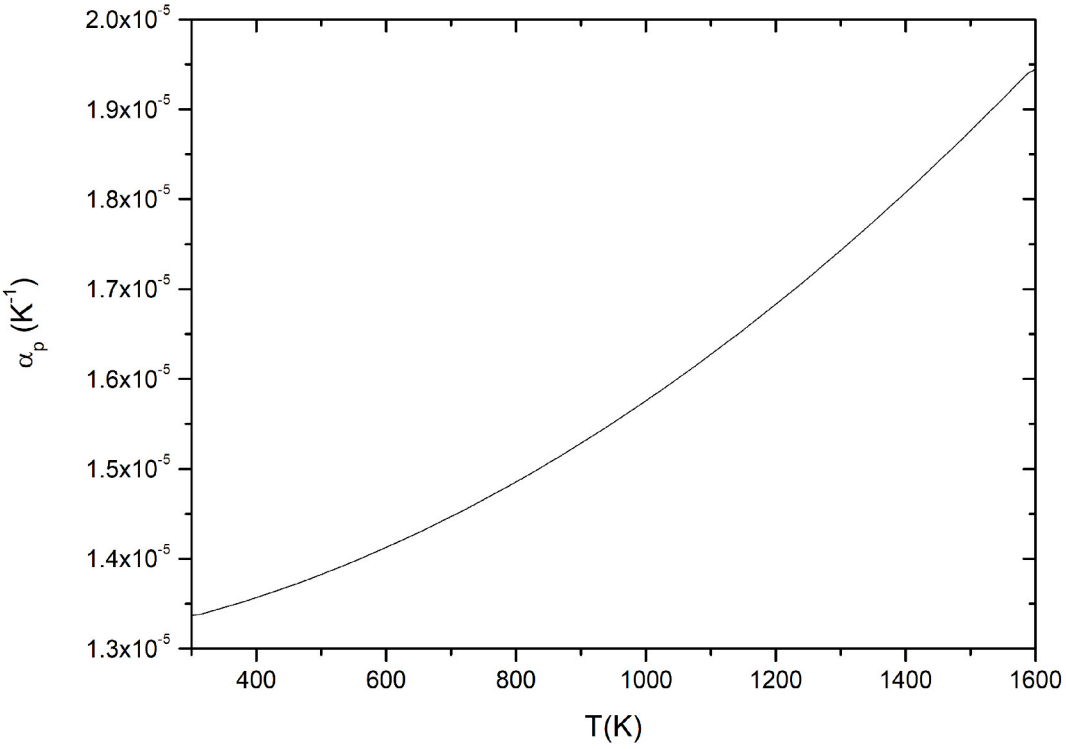


Fig. 3. Linear thermal expansion coefficient versus temperature.

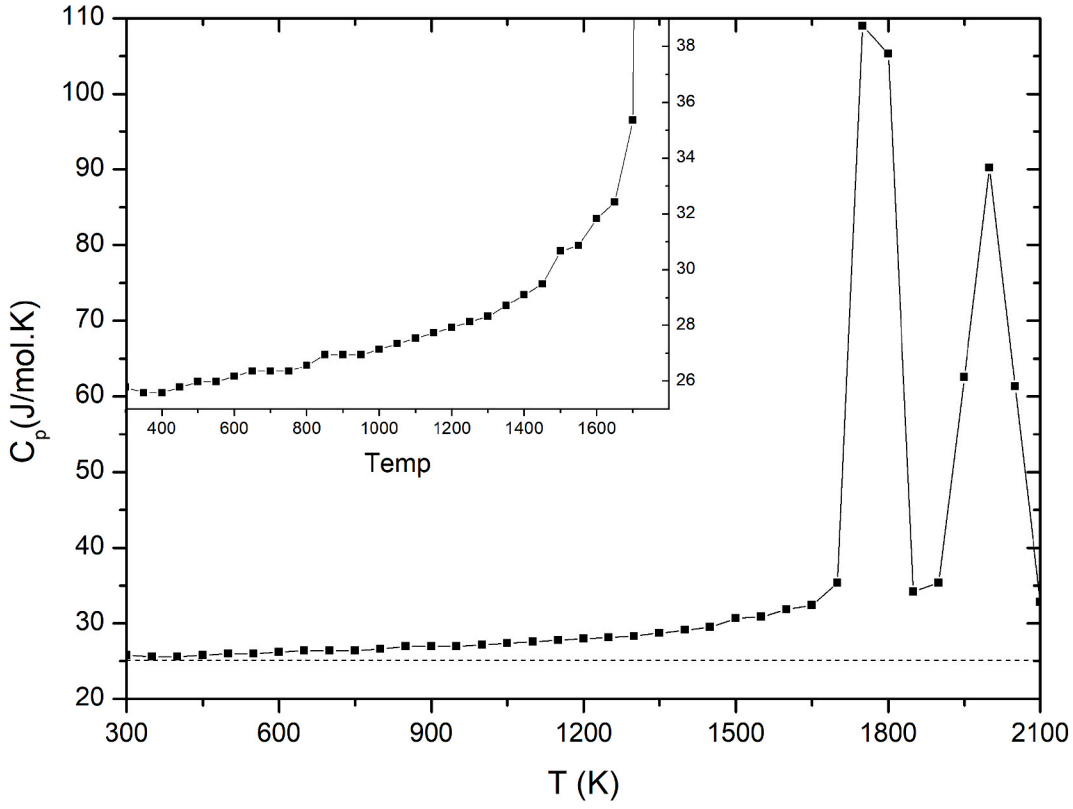


Fig. 4. Constant pressure specific heat of magnesium arsenide versus temperature.

as far as to our knowledge, there is no experimental data on thermal expansion coefficient of magnesium arsenide.

3.2.3. Specific heat

Specific heat data were calculated from the total energy of the MD supercell at constant pressure and were given in Fig. 4.

$$C_p(T) = \left(\frac{\partial E}{\partial T}\right)_p \tag{12}$$

Specific heat is constant, and it is about ~25 J/mol.K at room temperature, which is known from classical physics (Dulong-Petit law). Specific heat data, C_p, gradually increased with temperature (300 K–1800 K). Enhancement in data generally interpreted as an increase in the vibration of atoms. Numerical data from MSD show that the amount of vibration increases with temperature (see section 3.2.5).

Enthalpy change data displayed two discontinuities at the superionic phase transition and the melting points (see Fig. S1 in the supplementary material). The specific heat values in Fig. 4 displayed two sharp peaks. The superionic phase transition and the melting point were between 1750 K-1800 K and 1950 K–2000 K, respectively. These values are in agreement with the data in Section 3.2.1.

3.2.4. Radial distribution function

The radial distribution function is an essential structural data characterizing crystal, amorphous and liquid structures. It demonstrates the information on how ions are radially packed around a central ion. It also displays the density distribution from a reference point. Some quantitative data can be derived from the radial distribution data, like nearest neighbor distances and coordination numbers. Five different temperature data were presented to recognize the differences amongst each peak in Fig. 5. Sharp peaks broadened and fluctuations occurred around "1" with the increase in temperature. The first coordination number of ions were calculated as $N_{As-Mg} = 6, N_{Mg-As} = 4$, $N_{As-As} = 6$, $N_{Mg-Mg} = 5$ from the radial distribution functions at room temperature (see Fig. S2

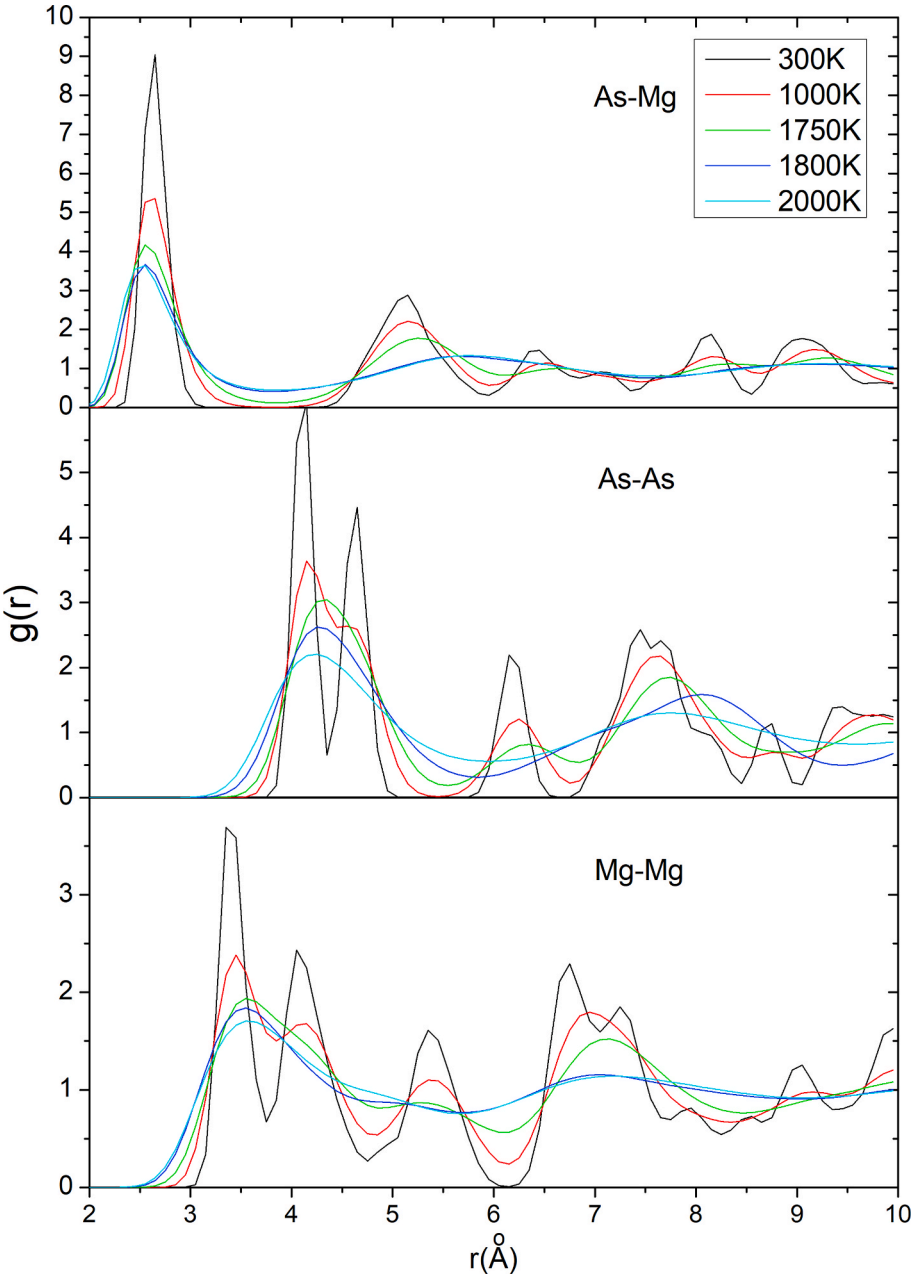


Fig. 5. Radial distribution functions of magnesium arsenide at five different temperatures.

in the supplementary material).

$$N = 4\pi \int_0^{r_1} r^2 g(r) \rho dr \tag{13}$$

The limits of the integral were from the origin to the first minimum following the primary peak of the radial distribution function. The first and the second coordination peaks of As–As gradually merge into one peak at about 1750 K–1800K in Fig. 5. The coordination numbers were recalculated from the principal peak and were found $N_{As-As} \approx$ 14at 1800K which is typical to the sum of the first two coordination numbers (8 +6) of a bcc structure (see section 3.2.7). Since the bcc structure is distorted at high temperatures, the principal peak of the As–As radial distribution function at the superionic phase (1800 K–1950 K) hosts the first and the second nearest atoms. It is also understood that the Mg structure, g_{Mg-Mg}, behaves like a liquid at 1800K compared to the radial distribution function data at the melting temperature. Both data are almost the same and oscillate around 1. This is an indication that there is a superionic transition.

3.2.5. *Mean square displacement and diffusion*

The motion of individual ion does not follow a straight line in a crystal structure, collisions of other ions divert the ion from its path. This motion can be described as a random walk and designated by Einstein formula,

$$\Delta r^2 = 6Dt + C \tag{14}$$

It is inferred from equation (14) that the elapsed time of an ion in a crystal is related to its mean square displacement. D and C are constants where D is the diffusion coefficient.

Mean square displacement within the first ~0.1–0.2 ps displayed a parabolic behavior for both anions and cations in Fig. 6. Displacement of an ion with time had a linear relationship before the first collision takes place, which means at the beginning ion had almost constant velocity. Beyond this point, in the solid phase, mean square displacement data remained constant with time. Ions leave their normal positions and begin to diffuse at elevated temperatures where mean square displacement data has a non-zero slope.

$$\Delta x^2 = 2D_x t + C_x,$$

$$\Delta y^2 = 2D_y t + C_y, \tag{15}$$

$$\Delta z^2 = 2D_z t + C_z$$

$$D = \left(D_x + D_y + D_z\right) / 3 \tag{16}$$

Self-diffusion coefficients of the Mg_3As_2 were determined from the slope of the mean square displacement data by equation (14). Since we were also concerned with diffusion constants for each axis, they were calculated and averaged by (equations 15 and 16). A gradual increase was observed in self-diffusion coefficient data for both magnesium and arsenic ions with temperature from room temperature to 1300 K (Fig. 7). They both decreased in the temperature range of 1300 K–1400 K. They jointly rose again from 1400 K to 1750 K and decomposed at 1800K. Mg ion diffusion coefficient increased rapidly compared to As ion and displayed liquid behavior at 1800 K. This indicated that the superionic phase transition took place in a way to support our assumptions in previous sections.

Self-diffusion coefficients in three dimensions are uniform for a cubic crystal. Components of diffusion data in x, y and z-direction showed fluctuations and were almost the same between 300 K and 1300 K. However, z component is about an order of magnitude higher than the x

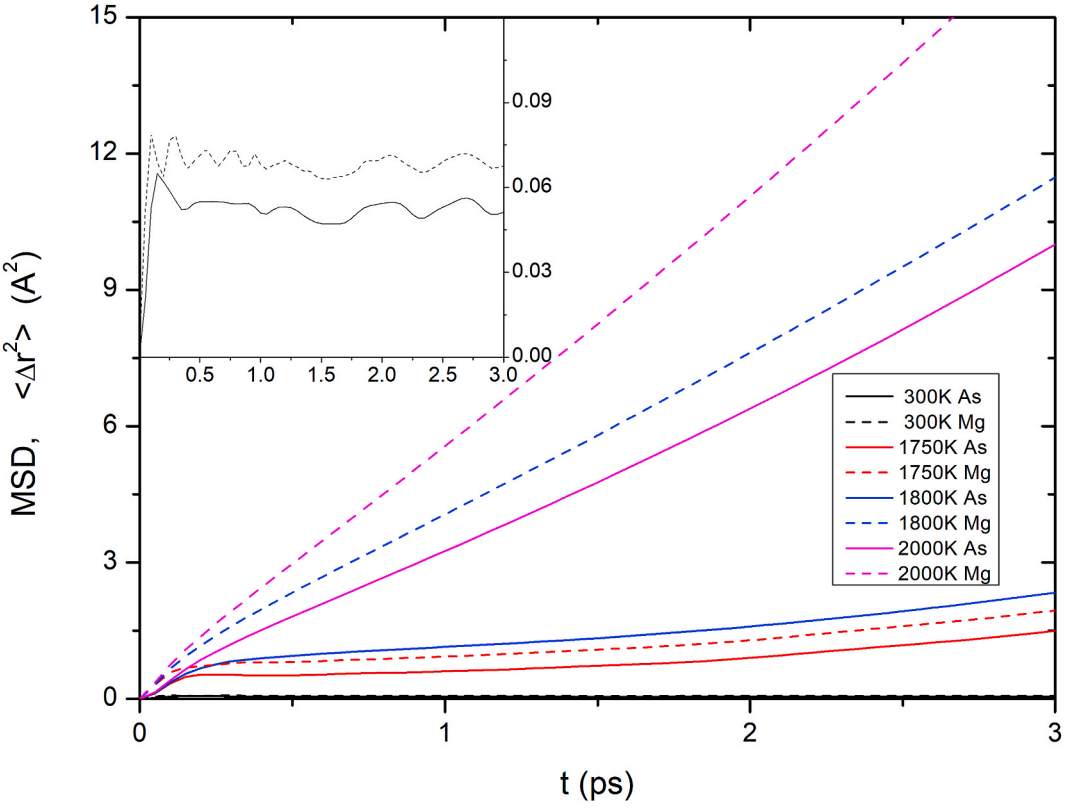


Fig. 6. Mean square displacement data at various temperatures.

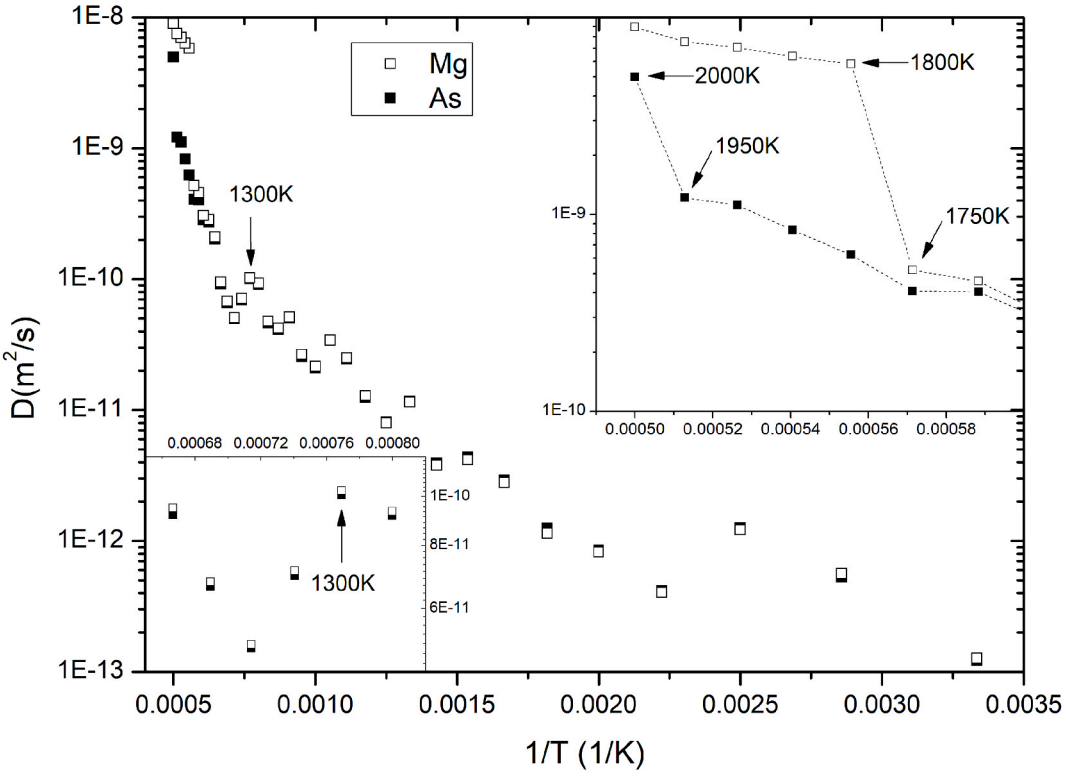


Fig. 7. Self-diffusion coefficients of magnesium arsenide versus temperature.

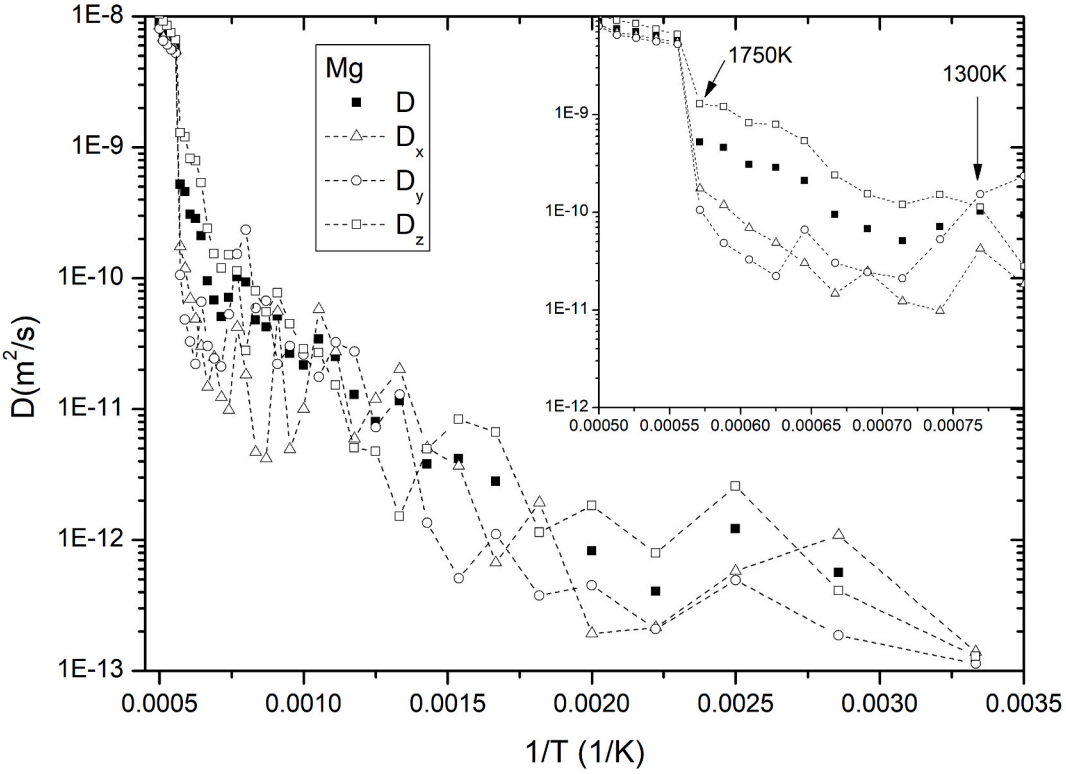


Fig. 8. Self-diffusion components of magnesium versus temperature in magnesium arsenide.

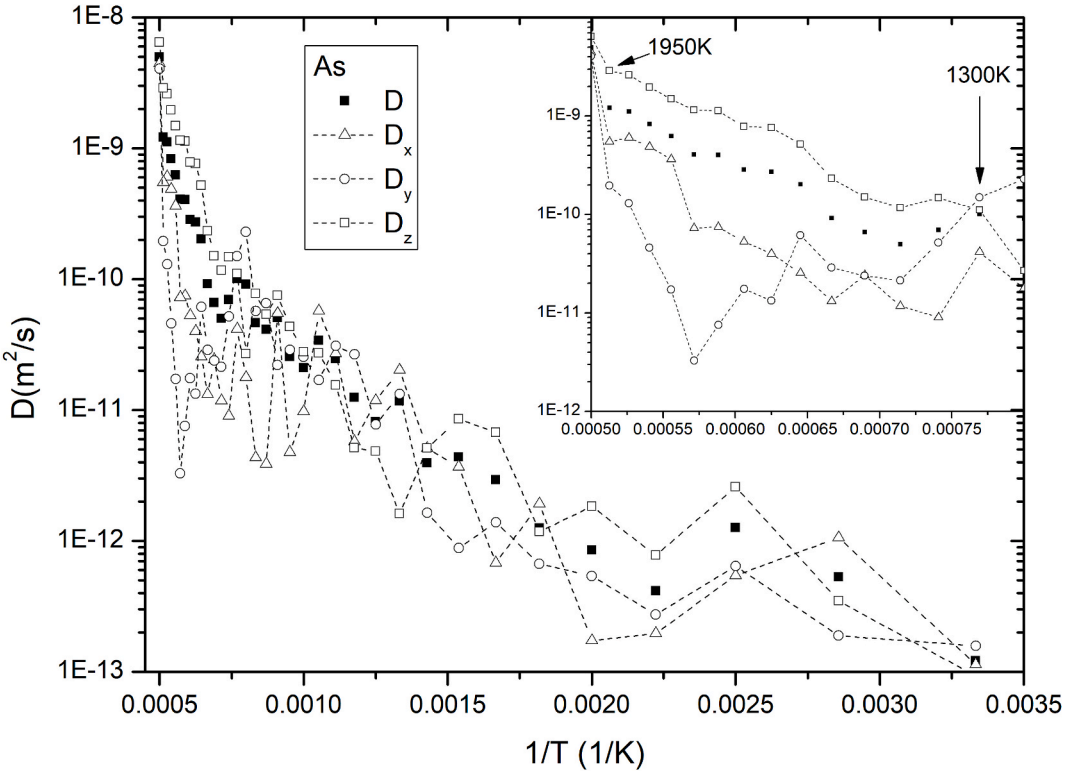


Fig. 9. Self-diffusion components of arsenide versus temperature in magnesium arsenide.

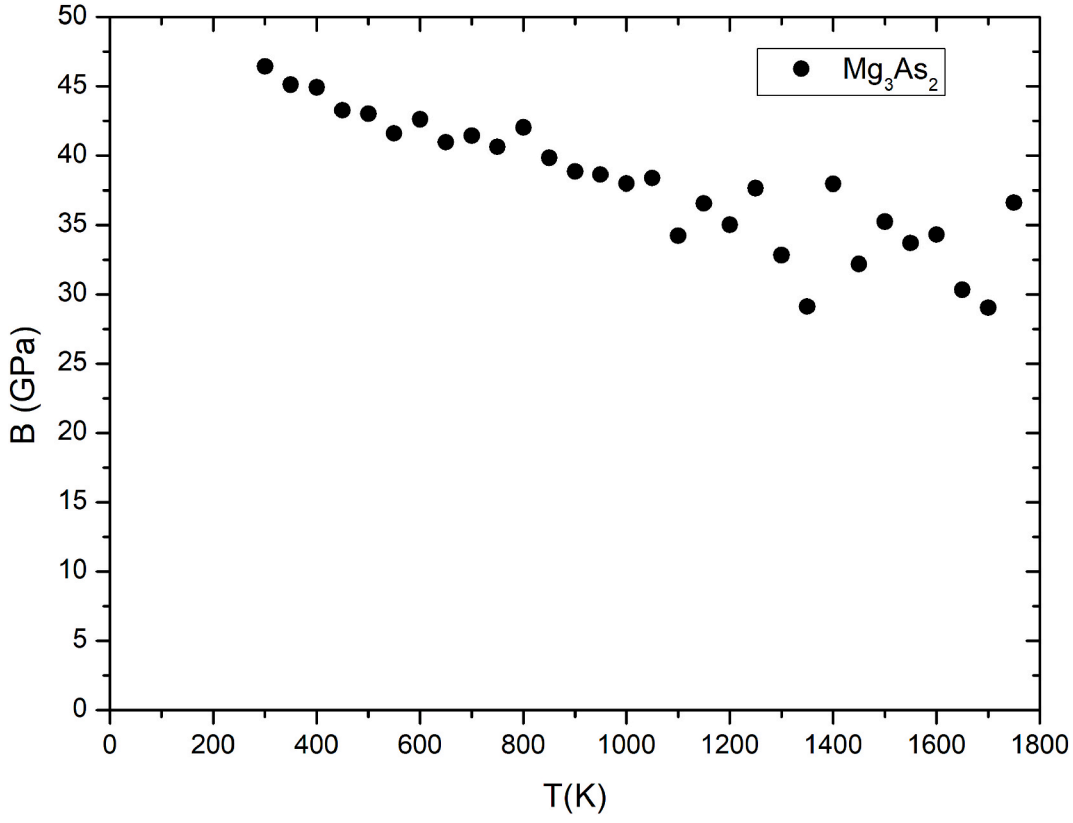


Fig. 10. Bulk modulus value of magnesium arsenide versus temperature.

and *y* components from 1350 K to the superionic transition temperature for Mg (Fig. 8) and 1350 K to the melting point temperature for As (Fig. 9).

When crystal structures undergo an allotropic phase transition, physical properties could change. Components of the self-diffusion data could demonstrate the presence of the structural phase transition. Some structural transitions may be accompanied by a decrease or an increase in the self-diffusion data [24]. In Fig. 7, between ~1300 K and 1400 K self-diffusion coefficients of Mg and As display a decrease. Besides, the large difference between the z component and x, y components of the diffusion constants above 1300K for both Mg and As ions resembles diffusion values of hexagonal structures. In general, a hexagonal structure has two principle diffusion components, one is perpendicular to the axis $D_{\perp} = D_x = D_y$, and the other is parallel to the axis $D_{\parallel} = D_z$. It is typical that one is greater than the other ($D_{\parallel} > D_{\perp}$) for hexagonal structures [24]. Experimental studies reveal that Mg_3As_2 has a high-temperature phase structure, which is a hexagonal, from 1273 K −1373 K to the melting point. Even if structural data of the crystal obtained from simulation did not display the transition from cubic to hexagonal structure (see section 3.2.1), it suggests that the interaction potential tends to transform the system over 1300 K.

3.2.6. Isothermal bulk modulus

The isothermal bulk modulus of a crystal structure was calculated by applying several different hydrostatics pressures around each equilibrium lattice points. The intended property was calculated from the derivative of these pressure-volume data of each temperature from 300 K up to 1750 K,

$$B_T(T) = -V(T)\left(\frac{\partial P}{\partial V}\right)_T \tag{17}$$

Standard deviation values in pressure data comprise too much oscillation. The supercell size was increased to 6 × 6 × 6 where the total number of ions is 17280 (6912 As^{-3} and 10368 Mg^{+2}) to minimize the uncertainty.

Bulk modulus versus temperature data demonstrate almost a linear dependence (Fig. 10) which could be described as,

$$B(T) = B_o + cT \tag{18}$$

B_o was calculated from equation (18) as 47.94 GPa by fitting data in Fig. 10, which is almost equal to the static calculations (47.109 GPa) in section 3.1. *c* constant is −0.00967 GPa × K^{-1}. Isothermal bulk modulus value displays a gradual decrease from 45.04 GPa to 31.02 GPa as the temperature was increased from 300 K up to 1750 K using equation (18).

3.2.7. Powder diffraction pattern

Simulation of powder diffraction pattern had been performed with the VESTA program [25] for Mg_3As_2 structure at various temperatures. The wavelength was chosen as 1.54059 Å and as a result, the intensity versus 2θ data was calculated (Fig. 11). Primarily, the simulation box in an equilibrium state at room temperature was examined, and the input structure was shown to be preserved. Diffraction data of equilibrated simulation boxes at 1750K and 1800K were compared to observe the structural change occurring during solid-superionic phase transition. The diffraction pattern of the structure at 1800K was analyzed with the help of Match! program. It was observed that the structure transformed from $Ia\bar{3}$ to $Im\bar{3}m$ space group, a cubic bcc unit cell. Diffraction data and visual investigations showed that magnesium sub-lattice collapsed, and only arsenic was solid in the superionic phase. Finally, the equilibrated simulation box at 1950K was examined to show that the structure obtained at 1800K was preserved to the melting temperature. Data obtained with both simulation programs (MD_1, MD_2) confirm this transition (see Fig. S3 in the supplementary material). The presence of the bcc cubic structure was demonstrated by visual inspections of the MD simulation box (see Fig. S4 in the supplementary material) (Video 1).

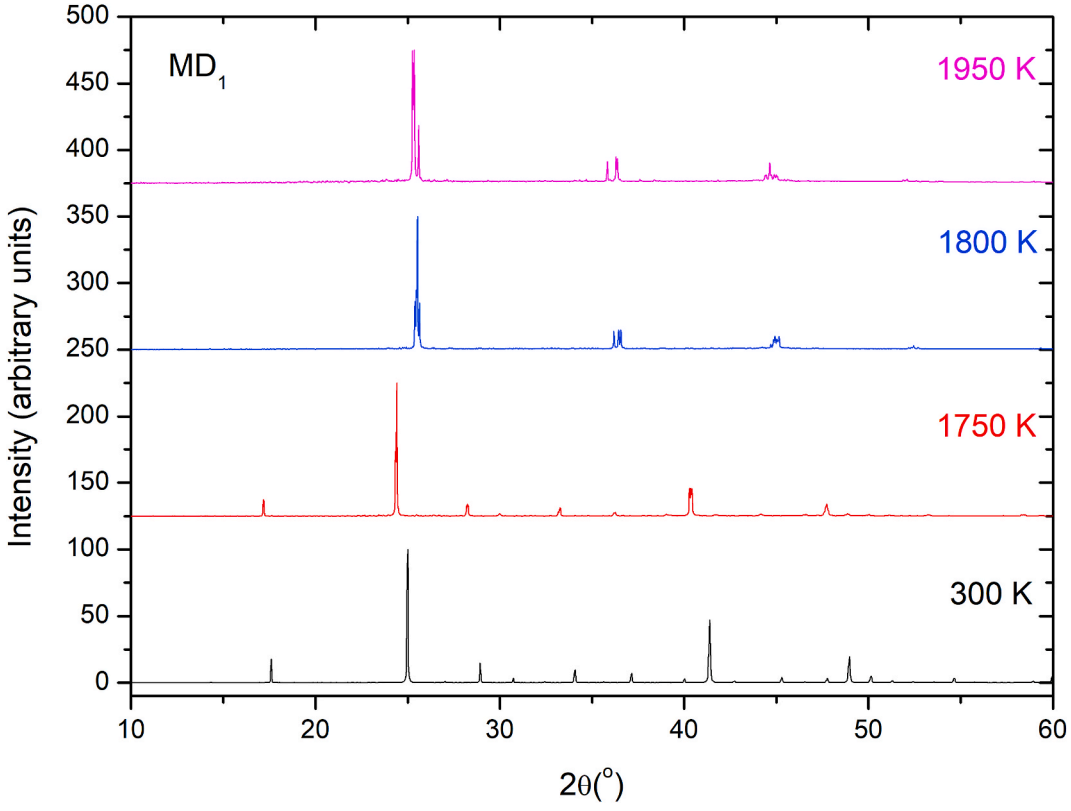


Fig. 11. Powder diffraction pattern of magnesium arsenide at various temperatures.

3.2.8. Determination of phase transition temperatures with two-phase simulation method

3.2.8.1. Determination of melting point

3.2.8.1.1. Solid – liquid box. Gradual heat treatment on the crystal structure from the solid to the liquid phase generally results in an overestimation of melting temperature in molecular dynamics simulation. The main reason for this is the lack of nucleation of the liquid phase in the simulation cell. An overheated simulation box with a one-phase crystal structure does not melt until it cannot sustain shear stress. The same problem occurred in this study in previous sections, and the melting point was calculated as ~2000K with a one-phase simulation box. To obtain the "correct" melting point of a material with the present potential parameters, an equilibrated simulation box should be acquired with both liquid and solid phases coexist at the same temperature. Initially, two independent simulations were performed at 300K and 2000K. These equilibrated simulation boxes were placed side by side, solid and liquid, in one simulation box for the initial structure. NPH ensemble was applied to the supercell, so the temperature of the system inherently evolve to the melting point where both phases coexist (see Fig. S5 in the supplementary material). Liquids tend to dilate non-uniformly; to avoid this, isotropic constant pressure method was used. Hydrostatic pressure was applied to the MD_2 simulation box.

When the temperature of the simulation is below the melting point while the simulation is in progress, the solid-liquid interface starts to move toward the liquid phase and a significant portion of the system solidifies. However, the two-phase state can still be maintained (see Fig. S6 in the supplementary material). If the system energy is too low, then the interface will disappear, and the total solidification takes place. Total liquefaction occurs if the system energy is too high. MD simulations were performed with initial temperatures between 1800 K and 2150 K, and in most of them two-phase coexist at the end of MD runs (see Table S1 in the supplementary material). The melting point temperature was calculated ~1562 K. This value will be corrected in the next section.

3.2.8.1.2. Superionic – liquid box. In reality, when the temperature gradually increased, adjacent phases at the melting point for Mg_3As_2 is not solid-liquid, but rather superionic-liquid. Therefore, the superionic and the liquid simulation boxes were combined, and simulations were performed (see Figs. S7–S11 in the supplementary material). The melting point temperature was calculated ~1700 K (see Table S2 in the supplementary material).

3.2.8.2. Determination of superionic phase transition point

3.2.8.2.1. Solid – superionic box. The physical parameters obtained with the current interaction potential have shown that Mg_3As_2 has a superionic phase above a certain temperature value. When we examine the enthalpy change data at the solid-superionic transition point (see Fig. S1 in the supplementary material), although the energy was transferred to the system, the temperature had changed so little that it had remained almost constant. There is a discontinuity in the enthalpy - temperature curve. The solid-superionic phase transition is a first-order phase transition. The energy given to the system during the phase transition is used to break the bonds between magnesium atoms. The magnesium sub-lattice has transformed from a solid phase to the liquid phase. Such a transition contains latent heat (heat of transformation).

A solid-liquid phase transition also contains latent heat (heat of fusion). In the literature and this study, MD simulation boxes with two different phases were used to find the melting temperature of the system. The superionic phase transition temperature could also be calculated by combining the solid-superionic box using the same method due to such similarity. (see Figs. S12–S16 in the supplementary material). The superionic phase transition temperature was found to be ~1505 K (see Table S3 in the supplementary material).

3.3. Discussion

In the present study, classical molecular dynamics and first-principles methods were used to investigate the Mg_3As_2 crystal structure. Buckingham type semi-empirical interionic potential model was proposed for classical MD simulations of Mg_3As_2. Potential parameters were estimated by fitting to available first-principles and experimental data in the literature. As far as to our knowledge, all computational data in the literature were calculated in the ground state with the first-principles method. Experimenters measured some physical properties at various temperatures such as room temperature lattice parameter (12.33 Å), crystal structures, structural phase transition temperature (1273 K–1373 K), and the melting point ($T_m > 1473\ K$).

The potential parameters were implemented in three different classical molecular dynamics programs. Elastic constants, bulk modulus, shear modulus, Young's modulus, Poisson's ratio, anisotropy factor, compressibility, and lattice parameter were predicted at 0 K by classical methods. Thermodynamic properties such as lattice parameters, linear thermal expansion coefficients, heat capacities, bulk moduli and diffusion coefficients with temperature were calculated. The room temperature lattice parameter was predicted as 12.329 Å by classical MD simulation. The superionic transition and the melting points were detected from the lattice parameter, energy (heat capacity), and mean-square displacement (diffusion) data as ~1800K and ~2000 K, respectively. Since the present simulation was a one-phase simulation, the superionic transition and the melting points were overestimated. A general solution to this problem is performing two-phase simulations with various initial temperatures close to the phase transition points. The instantaneous temperature tends to approach the melting point during the NPH ensemble simulation. Two-phase should be observed in the simulation box at the end of a relatively long run. Superionic and melting phase transition points with the present interaction potential were $T_c = 1505\ K$ and $T_m = 1700\ K$, respectively.

In literature, magnesium arsenide undergoes an allotropic transformation from cubic Mn_2O_3 to hexagonal anti-La_2O_3 system. The transformation was not observed with the present interaction potential parameters. First-principles calculations had also been performed. Ground state properties such as lattice parameter and bulk modulus values were attained, and the results were quite similar to the data in the literature.

4. Conclusion

The allotropic (cubic-hexagonal) transformation observed with the experiment cannot be obtained in the MD simulation, however, diffusion constants along each of the axes behaves similarly to a hexagonal structure rather than a cubic structure from 1350 K to phase transition temperatures (superionic and melting). This gives us a clue that the interaction potential tends to form the structural phase transition. Therefore, some changes can be made to classical MD simulation to observe a structural phase transition in future studies. 1) Fine adjustments can be made with the simulation input parameters 2) Minor changes can be made to the interaction parameters or new components can be added to the potential function 3) Alternative computer experiments can be performed with existing interaction parameters.

The difference between two separate computer simulation experiments on the melting point is almost 150 K in section 3.2.8.1. The most important reason for this is that the Mg sub-lattice collapses and loses a large amount of energy at the superionic transition temperature. Besides, As sub-lattice undergoes a structural change. These incidents affected the results of computer experiments designed to find the melting temperature. Combining solid-liquid phases means to ignore superionic transition. If a Mg_3As_2 crystal is subjected to a slow heat treatment, the coexistence of the superionic-liquid phase is a more realistic approach than a solid-liquid case at the melting point. When

performing two-phase simulations at the melting temperature, the heat of transformation (if any) must be taken into account and the correct phases should be brought together.

In the literature, there is no information about the presence of a superionic phase transition at high temperatures for Mg_3As_2. However, due to the insufficient data at temperatures above 1473 K, such an assumption had been made. The superionic transition temperature was calculated as ~1505 K. Consequently, the superionic phase transition can occur at high temperatures where experimental data is not yet available, or this can only be an artificial event only due to the current interaction potential. The results need to be confirmed by experimental studies.

To the best of our knowledge, the superionic phase transition temperature was determined for the first time in this study by the two-phase MD simulation box method. Studies had been performed in the literature with superionic materials, and superionic transition temperatures were determined by the MD simulation method by gradual heating of one phase box. However, the difference between single- and two-phase simulation data is quite evident in this study, which is almost 300 K. It is understood from this study that calculations involving especially type-I superionic materials [26] need to be revised. Abrupt physical changes occur in this type of superionic materials, resulting in a rapid increase in diffusion, ionic conduction and energy.

In this work, thermophysical properties of magnesium arsenide successfully reproduced with newly proposed potential parameters, which demonstrates that these potential parameters are robust both at low and high temperatures. Consequently, the present potential provides a good description of magnesium arsenide crystal.

CRediT authorship contribution statement

Seçkin D. Günay: Conceptualization, Investigation, Methodology, Visualization, Writing - original draft, Writing - review & editing, Funding acquisition, Project administration.

Declaration of competing interest

The authors declare that they have no known competing financial interests or personal relationships that could have appeared to influence the work reported in this paper.

Acknowledgements

The numerical calculations reported in this paper were partially performed at TUBITAK ULAKBIM, High Performance and Grid Computing Center (TRUBA resources). Computing resources used in this work were partially provided by the National Center for High Performance Computing of Turkey (UHeM) under grant number 5003802015. This work was supported by Research Fund of the Yildiz Technical University. Project Number: FBA-2018-3424.

Appendix A. Supplementary data

Supplementary data to this article can be found online at https://doi.org/10.1016/j.jpcs.2020.109614.

References

[1] T. Kajikawa, N. Kimura, T. Yokoyama, Thermoelectric properties of intermetallic compounds: Mg_3Bi_2 and Mg_3Sb_2 for medium temperature range thermoelectric elements, Proceedings of the 22nd International Conference on Thermoelectrics (2003) 305–308, https://doi.org/10.1109/ICT.2003.1287510.
[2] K. Pigon, Uber die Halbleitereigenschaften des Magnesiumarsenides Mg_3As_2, Helv. Phys. Acta 41 (1968) 1104–1109, https://doi.org/10.5169/seals-113976.
[3] R.C. Ropp, Chapter 4 - group 15 (N, P, as, Sb and Bi) Alkaline aarth compounds, in: Encyclopedia of the Alkaline Earth Compounds, Elsevier, Amsterdam, 2013, p. 199, https://doi.org/10.1016/B978-0-444-59550-8.00004-1, 350.
[4] Y. Imai, A. Watanabe, Electronic structures of Mg_3Pn_2 (Pn=N, P, As, Sb and Bi) and Ca_3N_2 calculated by a first-principle pseudopotential method, J. Mater. Sci. 41 (2006) 2435–2441, https://doi.org/10.1007/s10853-006-5181-3.
[5] H. Zhang, S. Shang, J.E. Saal, A. Saengdeejing, Y. Wang, L.-Q. Chen, Z.-K. Liu, Enthalpies of formation of magnesium compounds from first-principles calculations, Intermetallics 17 (2009) 878–885, https://doi.org/10.1016/j.intermet.2009.03.017.
[6] A. Mokhtari, M. Sedighi, The effect of hydrostatic pressure on the physical properties of magnesium arsenide in cubic and hexagonal phases, Phys. B Condens. Matter 405 (2010) 1715–1720, https://doi.org/10.1016/j.physb.2009.12.075.
[7] S. Ganeshan, S.L. Shang, H. Zhang, Y. Wang, M. Mantina, Z.K. Liu, Elastic constants of binary Mg compounds from first-principles calculations, Intermetallics 17 (2009) 313–318, https://doi.org/10.1016/j.intermet.2008.11.005.
[8] J. Tani, M. Takahashi, H. Kido, Lattice dynamics and elastic properties of Mg_3As_2 and Mg_3Sb_2 compounds from first-principles calculations, Phys. B Condens. Matter 405 (2010) 4219–4225, https://doi.org/10.1016/j.physb.2010.07.014.
[9] F. Kayadibi, S.D. Günay, Ç. Taşseven, Studying static, dynamic and Transport properties of Mg_3Bi_2, Acta Phys. Pol., A 128 (3) (2015) 440–446, https://doi.org/10.12693/APhysPolA.128.440.
[10] Ü. Akdere, S.D. Günay, Ç. Taşseven, Ordering and diffusion in liquid magnesium antimonide (Mg3Sb2) from hypernetted-chain theory and molecular dynamics simulation, Ionics 1–7 (2018), https://doi.org/10.1007/s11581-018-2757-2.
[11] J.D. Gale, A.L. Rohl, The general utility lattice program (GULP), Mol. Simulat. 29 (2003) 291–341, https://doi.org/10.1080/0892702031000104887.
[12] R.W.G. Wyckoff, The Structure of Crystals, second ed., The Chemical Catalog Company Inc, New York, 1935 https://doi.org/10.1002/jctb.5000504413.
[13] K. Refson, Moldy: a portable molecular dynamics simulation program for serial and parallel computers, Comput. Phys. Commun. 126 (2000) 310–329, https://doi.org/10.1016/S0010-4655(99)00496-8.
[14] S. Plimpton, Fast parallel algorithms for short-range molecular dynamics, J. Comput. Phys. 117 (1995) 1–19, https://doi.org/10.1006/jcph.1995.1039.
[15] G. Kresse, J. Hafner, Ab initio molecular dynamics for liquid metals, Phys. Rev. B 47 (1993) 558–561, https://doi.org/10.1103/PhysRevB.47.558.
[16] G. Kresse, J. Furthmüller, Efficiency of ab-initio total energy calculations for metals and semiconductors using a plane-wave basis set, Comput. Mater. Sci. 6 (1996) 15–50, https://doi.org/10.1016/0927-0256(96)00008-0.
[17] G. Kresse, J. Furthmüller, Efficient iterative schemes for ab initio total-energy calculations using a plane-wave basis set, Phys. Rev. B 54 (1996) 11169–11186, https://doi.org/10.1103/PhysRevB.54.11169.
[18] W. Voigt, Lehrbuch der Kristallphysik, Teubner, Leipzig, 1928, https://doi.org/10.1007/978-3-663-15884-4.
[19] A. Reuss, Berechnung der Fließgrenze von Mischkristallen auf Grund der Plastizitätsbedingung für Einkristalle, Z. Angew. Math. Mech. 9 (1929) 49–58, https://doi.org/10.1002/zamm.19290090104.
[20] R. Hill, The elastic Behaviour of a Crystalline Aggregate, Proc. Phys. Soc. 65 (1952) 349–354, https://doi.org/10.1088/0370-1298/65/5/307.
[21] J.H. Li, S.H. Liang, H.B. Guo, B.X. Liu, Four-parameter equation of state of solids, Appl. Phys. Lett. 87 (2005) 194111, https://doi.org/10.1063/1.2128071, 1 – 194111 3.
[22] S.F. Pugh, XCII. Relations between the elastic moduli and the plastic properties of polycrystalline pure metals, The London, Edinburgh, and Dublin Philosophical Magazine and Journal of Science 45 (1954) 823–843, https://doi.org/10.1080/14786440808520496.
[23] S. Haussühl, Physical Properties of Crystals: an Introduction, John Wiley & Sons, 2008, https://doi.org/10.1002/9783527621156.
[24] H. Mehrer, Diffusion in Solids: Fundamentals, methods, materials, diffusion-controlled processes, vol. 155, Springer, Berlin, Heidelberg, 2007, https://doi.org/10.1007/978-3-540-71488-0.
[25] K. Momma, F. Izumi, VESTA 3 for three-dimensional visualization of crystal, volumetric and morphology data, J. Appl. Crystallogr. 44 (6) (2011) 1272–1276, https://doi.org/10.1107/S0021889811038970.
[26] S. Hull, Superionics: crystal structures and conduction processes, Rep. Prog. Phys. 67 (7) (2004) 1233–1314, https://doi.org/10.1088/0034-4885/67/7/R05.